

Supporting Information

Ambient Temperature Deposition of Gallium Nitride / Gallium Oxynitride From a Deep Eutectic Electrolyte, Under Potential Control

Sujoy Sarkar and S. Sampath

Experimental Section

Preparation of ternary molten electrolyte: Urea and acetamide were of AR (Analytical reagent) grade and obtained from SD Fine Chemicals, India. They were dried over molecular sieves for several days. $\text{Ga}(\text{NO}_3)_3$ was purchased from Aldrich, USA, and kept in a desiccator before use. The ternary eutectic was prepared by mixing of acetamide, urea and gallium nitrate at the molar ratio as given below. The electrolyte was prepared in a closed double walled glass vessel where the temperature was maintained by circulating hot water through the outer jacket. Acetamide (0.54 mole fraction) was melted at 82°C and urea (0.41 mole fraction) was dissolved in it. Upon further addition of $\text{Ga}(\text{NO}_3)_3$ (0.05 mole fraction) into the binary mixture, a single phase liquid was obtained that was cooled to ambient conditions. Subsequently, the room temperature molten liquid was stored under inert atmosphere for further use.

Characterization: Infrared spectroscopy was carried out in the transmittance mode (Perkin Elmer, Spectrum one model FT-IR) with the ternary melt dispersed in KBr pellet. Raman spectroscopy was carried out using FT-Raman (Perkin Elmer) spectrometer with incident laser wavelength of 1064 nm. Surface tension of the melt was determined by the pendant drop method using a Phoenix 300 SEO surface tension/contact angle analyzer attached to a CCD camera. Measurements at different temperatures were carried out with a hot stage controlled by an external PID controller. Specific conductivity measurements were carried out using a conductivity cell (Orion 3 star, Thermoelectron Corporation, USA) with a cell constant of 1.01 cm^{-1} . Dynamic rheological measurements at different temperatures were carried out using a rheometer (Anton Paar, USA) with ‘cone and plate’ geometry. X-ray diffraction (XRD) patterns were recorded using $\text{Cu K}\alpha$ ($\lambda = 1.5406\text{ \AA}$) radiation on Philips analytical X-ray BV (PAN analytical X’pert) instrument. The as-deposited gallium nitride was analyzed by scanning electron microscopy (SEM, Carl Zeiss ultra 55) equipped with energy dispersive X-ray analysis (EDAX). Transmission electron microscopy (TEM, JEOL 2100F at 200 kV) of the sample was carried out on a Cu grid. X-ray photoelectron spectroscopic (XPS) measurements were performed using Kratos Axis Ultra spectrometer with $\text{Al K}\alpha$ (1486.6 eV) as the source and the analysis of XPS data was carried out using XPSpeakfit4.1 freeware software. Micro-Raman and photoluminescence (PL) spectra were recorded using a LabRam HR spectrometer (Horiba Jobin Yvon, France) with a 514.5 nm Ar^+ (for Raman) and 325 nm HeCd (for PL) laser as sources of excitation with an acquisition time of 10 s and 5 s

respectively. Each experiment was carried out at least three to four times to check the reproducibility of the data.

Electrochemical characterization based on voltammetry and chronoamperometry was carried out on electrochemical system (Autolab, Netherlands or 660A, CHI, USA) with three electrode setup. Polycrystalline Au foil of area 1 cm^2 was used as the working electrode, platinum and Ag/AgCl (ternary melt) were used as counter and reference electrodes respectively. The Au electrode was cleaned using piranha solution followed by electrochemical cycling in acidic solutions. The electrochemical experiments were performed with the electrolyte kept under nitrogen atmosphere on a lab bench. The deep eutectic was prepared and kept under inert atmosphere for a day before it was used for deposition. The electrochemistry and deposition did not change even if the electrolyte was stored for several days (in the inert atmosphere) before use. The distance between the working and the reference electrode was kept at 0.5 cm.

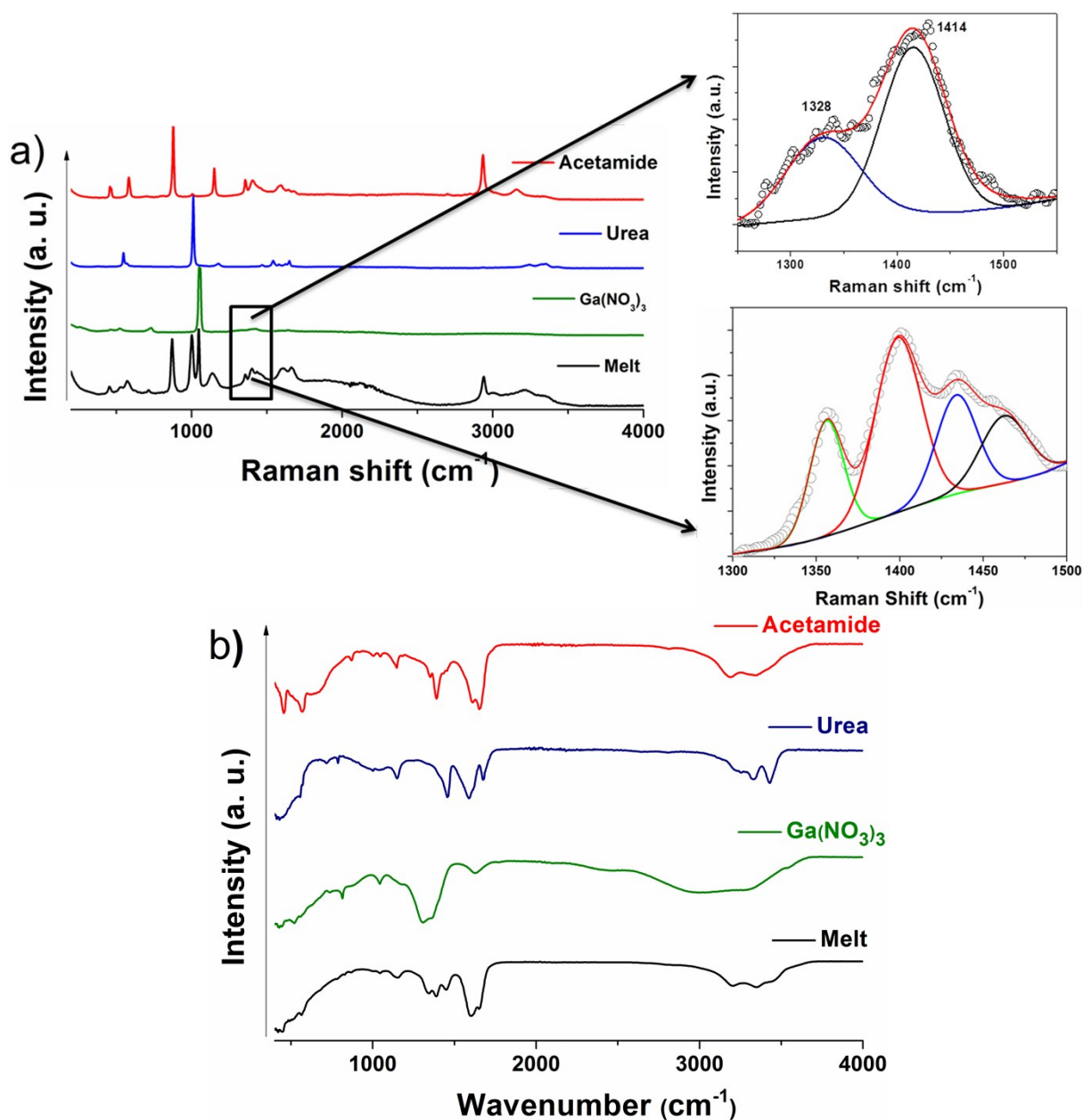


Figure S1. (a) Raman spectra and (b) FT-IR spectra of gallium nitrate containing ternary melt. The spectra of individual components namely, acetamide, urea, gallium nitrate are given for comparison. The spectra are artificially stacked for clarity.

Vibrational spectroscopic studies reveal (Fig. S1a) bands related to the components in the melt. The band observed at 1047 cm^{-1} corresponds to the symmetric NO_3^- stretch [$\nu_s(\text{NO}_3)$] of the free nitrate anion and the band at 1434 cm^{-1} corresponds to the anti-symmetric N-O stretch [$\nu_3(\text{NO}_3)$]. A closer look at the spectrum reveals an additional band at 1356 cm^{-1} which is due to NO_2 symmetric stretching in the melt.^{1,2} Appearance of additional bands and partial lifting of degeneracy of 1356 and 1434 cm^{-1} bands indicate a strong change in the geometry. The individual components, acetamide and urea have characteristic bands corresponding to NH, CN and C=O stretches that appear in the region between 1200 and 1800 cm^{-1} . Acetamide shows NH_2 deformation band at 1642 cm^{-1} (Table S1) whereas urea shows a deformation band at 1623 cm^{-1} . The Raman spectrum of the ternary melt shows a broad band in this region with simultaneous shift in the position of the NH_2 deformation band to 1606 cm^{-1} . The combination of acetamide and urea is expected to have extensive hydrogen bonding and the addition of gallium nitrate may possibly weaken the extent of hydrogen bonding by interacting with the NH_2 groups present in the base melt. This might result in band broadening with simultaneous shift in band positions observed for NH_2 deformation modes. Shifts in band positions as well as broadening are observed for C=O and CN stretching modes as well. The region between 800 and 1200 cm^{-1} also shows similar observations (Table S1). A strong-CN symmetric stretching band appearing at 1012 cm^{-1} for urea shows little broadening in the gallium nitrate containing melt suggesting possible interactions of nitrate anion with the other components of the melt (Table S1).

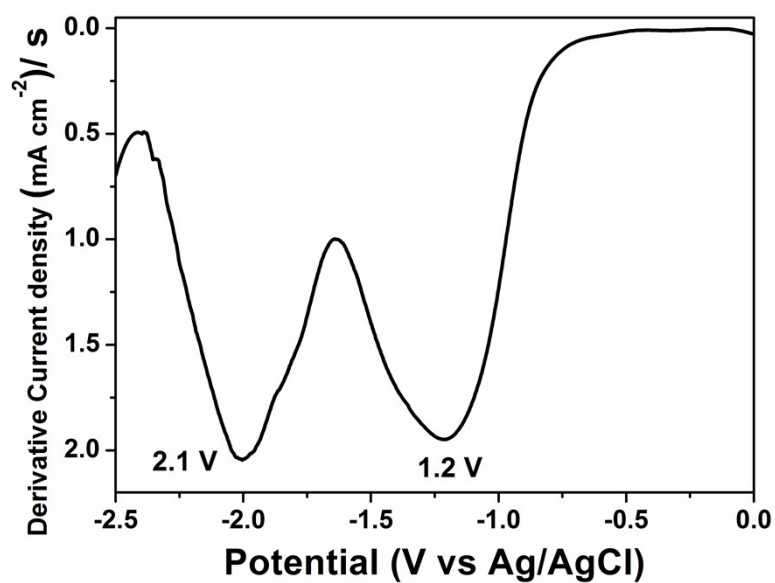


Figure S2. First order derivative current density vs. potential curve of the cyclic voltammogram displayed in figure 2a. The potential values indicated are the midpoint potentials of the reduction processes observed in the cyclic voltammogram.

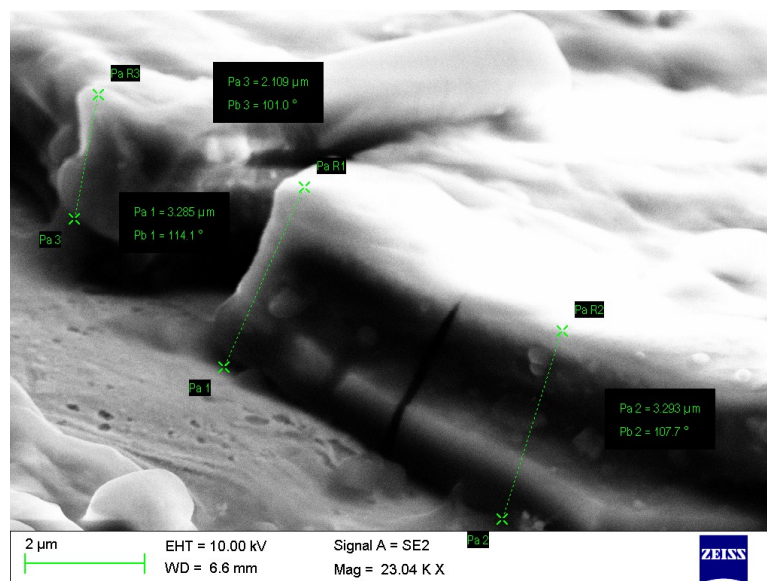


Figure S3. Cross-Sectional SEM image of the as-deposited gallium nitride on gold electrode. The average thickness of deposition is $4 \pm 1 \mu\text{m}$.

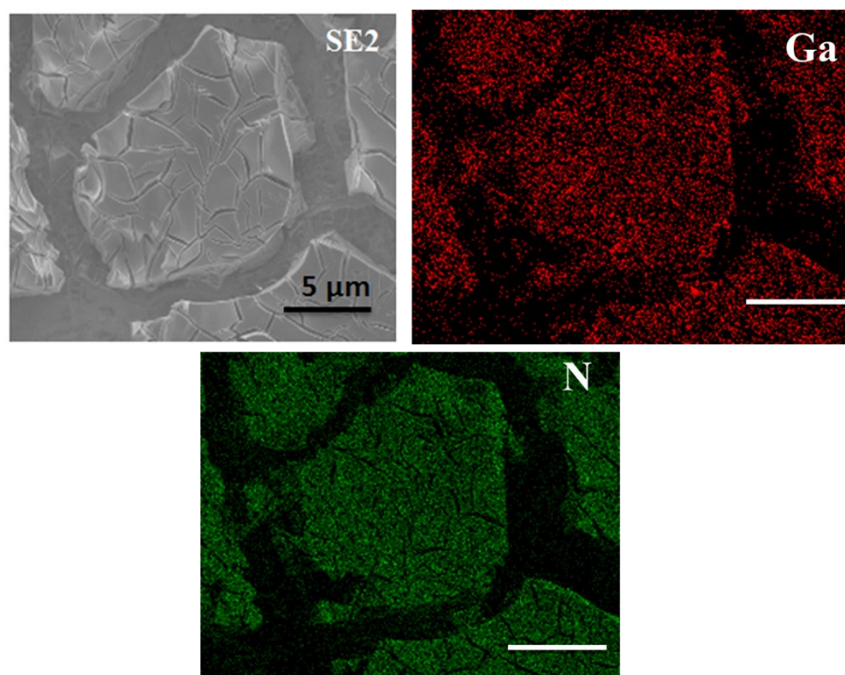


Figure S4. Secondary electron (SE2) image along with elemental mapping (Ga and N) of as-deposited gallium nitride. The scale bar is 5 μm .

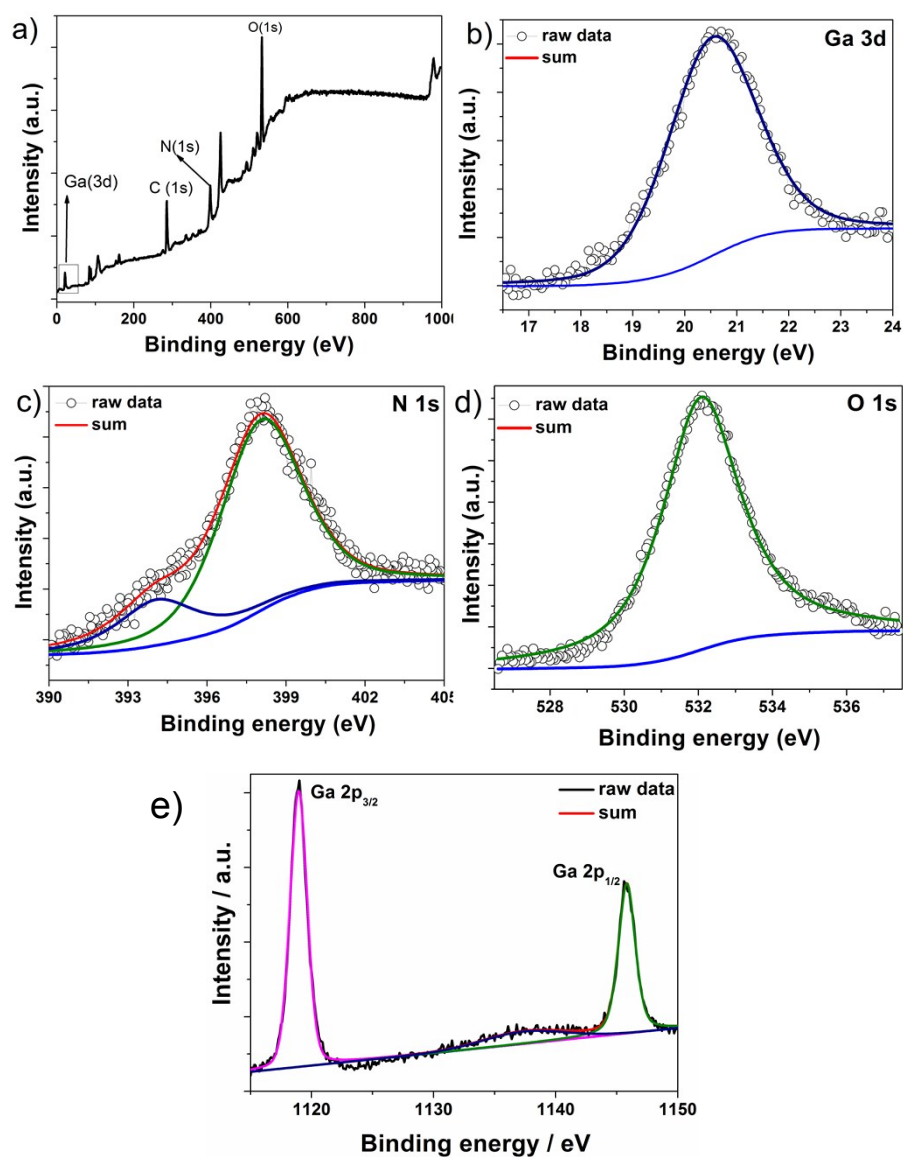


Figure S5. (a) XPS survey spectrum of the as-deposited gallium nitride film and the deconvoluted (b) Ga 3d, (c) N 1s, (d) O 1s and (e) Ga 2p regions are shown as well. The experimental data points along with the sum of the spectra are given. The background correction is carried out and Shirley algorithm is used for deconvolution of the spectra.

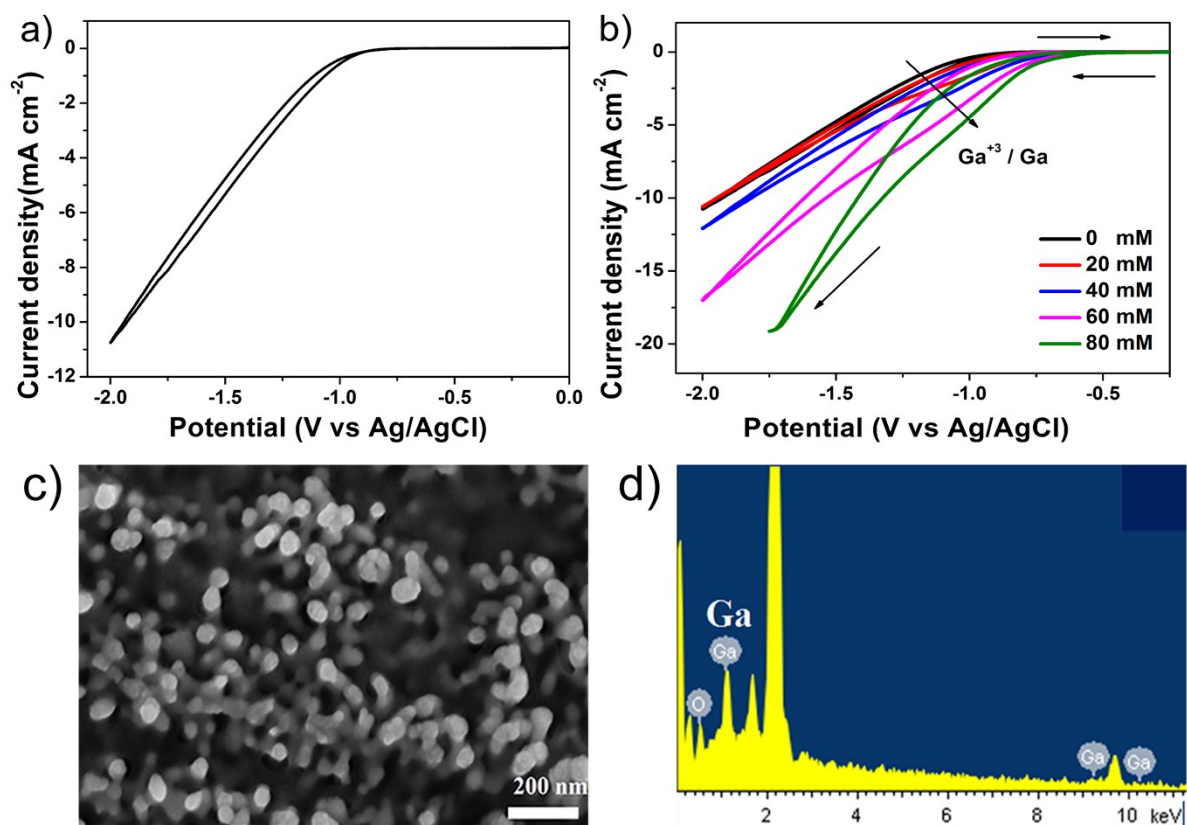


Figure S6. (a) Cyclic voltammogram of ammonium nitrate-based ternary melt on Au electrode at scan rate of 20 mVs⁻¹. (b) Cyclic voltammograms of ammonium nitrate-based ternary melt wherein different amounts of Ga(NO₃)₃ are added. Scan rate used is 20 mVs⁻¹. The numbers from 0-80 mM denote the concentration of Ga(NO₃)₃ in the melt. (c) The ESEM image of the as-deposited Ga on the substrate and (d) shows the corresponding EDS pattern.

High Temperature annealing of electrodeposited gallium nitride/gallium oxynitride

High temperature annealing of the as-deposited gallium nitride in presence of ammonia leads to highly crystalline wurtzite phase of GaN (Fig. S7, JCPDS no. 76-073). The morphology and elemental mapping of annealed GaN (Fig. S8) shows the flaky nature and there is no change observed before and after annealing. Fig. S9 shows the TEM images of the annealed sample, under NH_3 at 900°C , at different magnifications. The annealed sample contains nanoparticles of GaN with average size 5–10 nm. The SAED pattern reveals spots and rings corresponding to different facets, implying the presence of highly crystalline nanoparticles of GaN. The ring pattern is indexed to the hexagonal wurtzite GaN. The HRTEM indicates d-spacing of 0.275 nm corresponding to the (100) reflection of GaN. The deconvoluted core level XPS spectrum of Ga 2p and N 1s regions are shown in Fig. S10. The Ga $2p_{1/2}$ shows a binding energy of 1143.4 eV while N 1s shows a peak at 396 eV which is a sign of the presence of nitridic (N^{3-}) nitrogen and Ga-N bond. The difference in the peak position of nitridic nitrogen between the as-prepared and annealed samples show that the oxygen present is removed when annealed at 900°C in presence of ammonia. The atomic ratio of Ga $2p_{3/2}$ and N 1s is found to be 1.07 which is close to the stoichiometric GaN. Fig. S11 show the photoluminescence spectrum of GaN film after annealing at 900°C under NH_3 atmosphere. The band edge emission at 365 nm (3.4 eV) and a broad band at 650 nm (1.9 eV) close to the YB are observed. The blue band is not observed probably because of the removal of other oxygen containing compositions at high temperatures during the annealing process. High intense band edge emission implies that annealing improves the crystallinity and quality of the GaN.

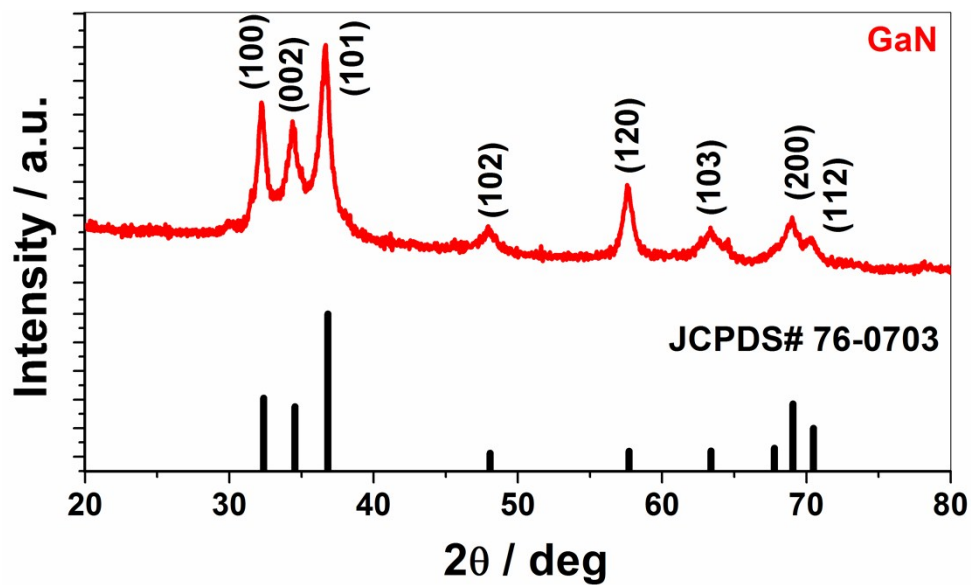


Figure 7. Powder X-ray diffraction pattern of the electrodeposited gallium nitride annealed at 900 °C in NH₃ atmosphere. The standard diffraction pattern for hexagonal wurtzite GaN (JCPDS No. 76-0703) is also given.

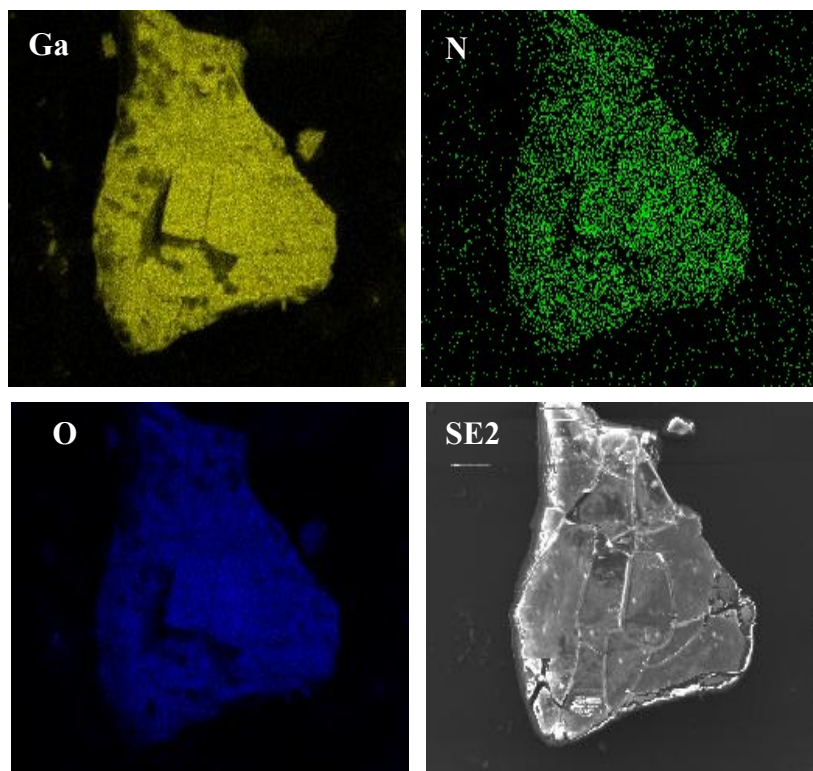


Figure S8. SEM micrographs along with elemental mapping of Ga, O and N for electrodeposited gallium nitride, annealed at 900 °C under NH_3 atmosphere.

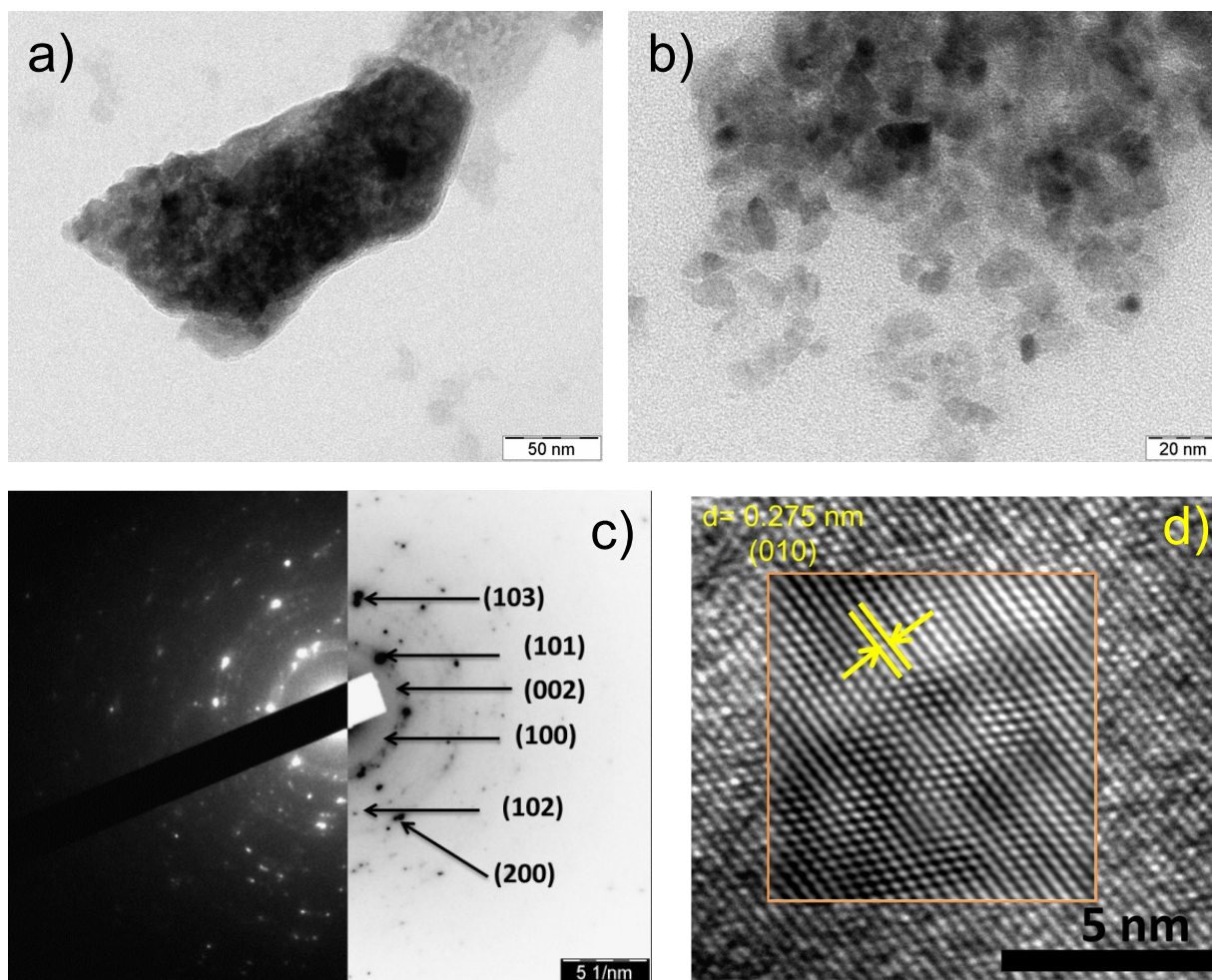


Figure S9. Bright filed TEM images (a, b) under different magnifications along with the indexed (c) SAED pattern and (d) HRTEM (inverse FFT of the marked region) of annealed gallium nitride.

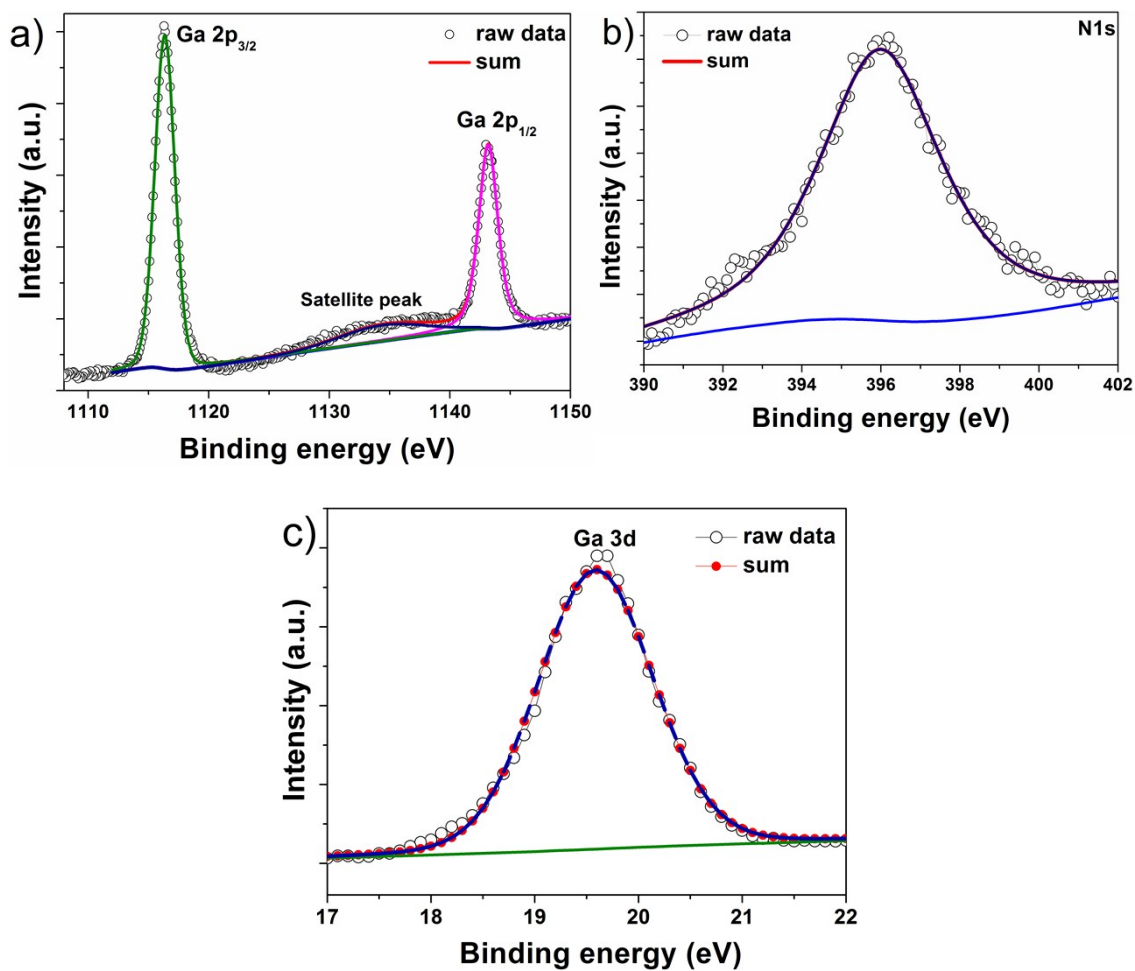


Figure S10. Deconvoluted XPS spectra of (a) Ga 2p, (b) N 1s and (c) Ga 3d regions of annealed gallium nitride.

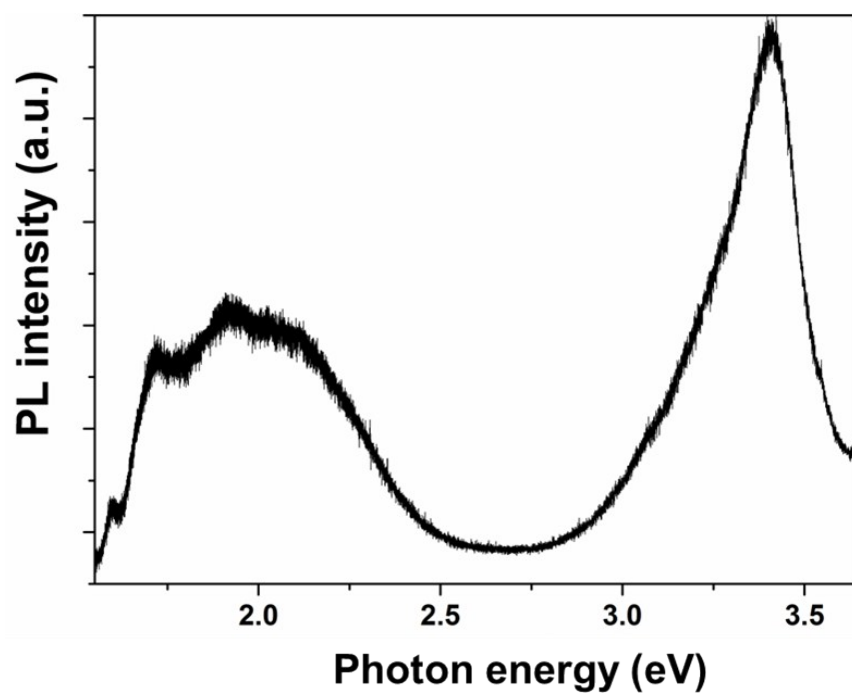


Figure S11. Photoluminescence spectrum of annealed gallium nitride. The excitation wavelength used is 325 nm (He-Cd laser).

In-situ Indium doping of In in gallium nitride phase

The bandgap engineering of as-deposited gallium nitride can be achieved by *in-situ* doping of indium into gallium nitride lattice. Preliminary studies using (0.1 %) of indium nitrate in the ternary eutectic containing acetamide, urea and gallium nitrate (Fig. S12) reveals the formation of composition containing In. A triple pulse sequence is used to deposit the material since In^{3+} can be very easily reduced and the pulse sequence is given in the caption of Figure S12. The SEM (Fig. S13) pictures reveal that the morphology of the electrodeposited material is not changed due to the incorporation of indium and the EDS and elemental mapping clearly shows the presence of very small amount of indium (0.5 atomic %). The corresponding XPS data (Fig. S14) shows the presence of core level In 3d peak. The deconvoluted spectrum of In core level shows the presence of two peaks at 445.7 eV and 453.3 eV corresponding to $3d_{5/2}$ and $3d_{3/2}$ levels respectively (Fig. S14), are close to the reported InGaN ,³ prepared by different physical techniques. The room temperature PL (Fig. S15) observed for the as-deposited In doped gallium nitride/oxy-nitride film shows a broad peak (FWHM >1 eV) appearing at 2.8 eV (~ 440 nm). The illumination of the material under UV light is captured through CCD camera and depicted as inset of Fig. S15. The PL maxima reported for InGaN phase⁴ are around 410 to 455 nm for samples with different thickness and different In content. The above preliminary results suggest that In could be incorporated into electrodeposited gallium nitride lattice forming InGa_xN_y .

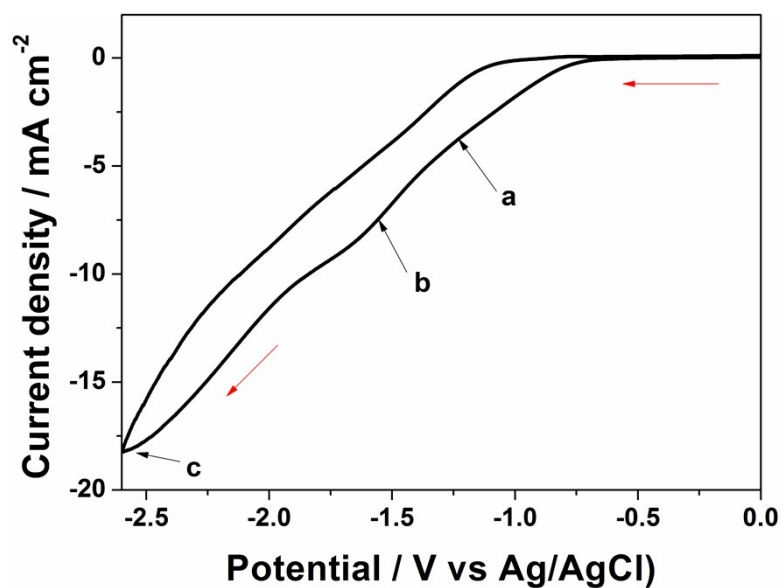


Figure S12. Cyclic voltammogram on Au electrode obtained in gallium nitrate based ternary melt containing 0.1 % of $\text{In}(\text{NO}_3)_3$. Scan rate used is 20 mV s^{-1} . Triple pulse amperometry at three different potentials, marked as ‘a’, ‘b’ and ‘c’, is used to deposit the material.

Point	Potential	time
a	-1.2 V	1 sec
b	-1.4 V	0.5 sec
c	-2.6 V	2 sec

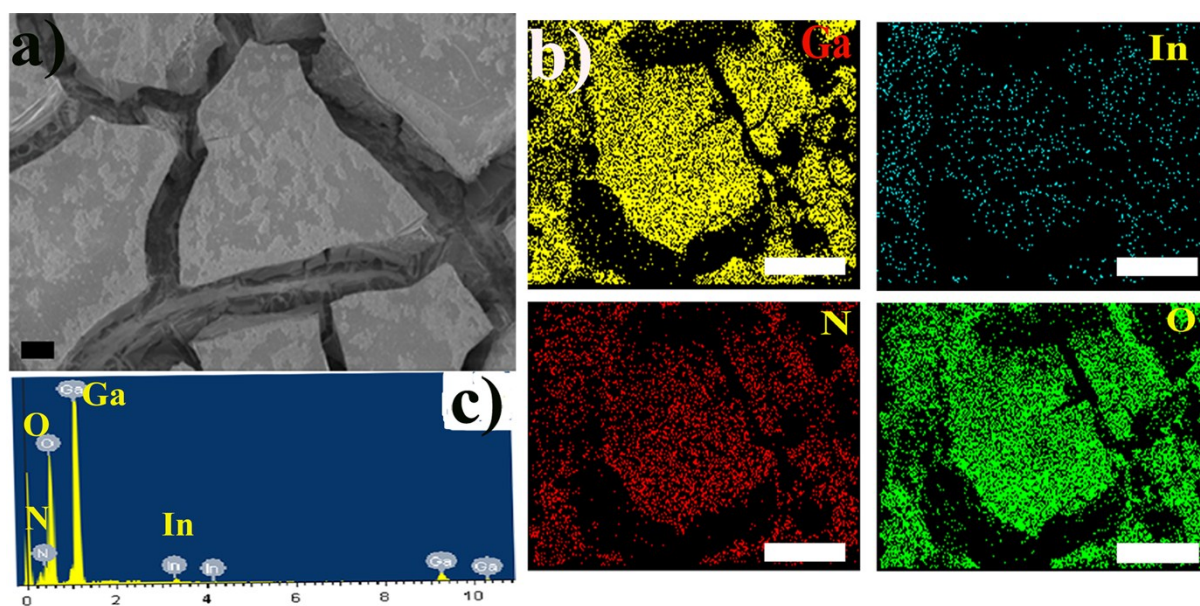


Figure S13. (a) FESEM micrographs of In doped gallium nitride film (scale bar : 5 μm); (b) Elemental mapping of Ga, In, N and O for the electrodeposited material (scale bar : 30 μm). (c) EDS shows presence of In, Ga, O and N.

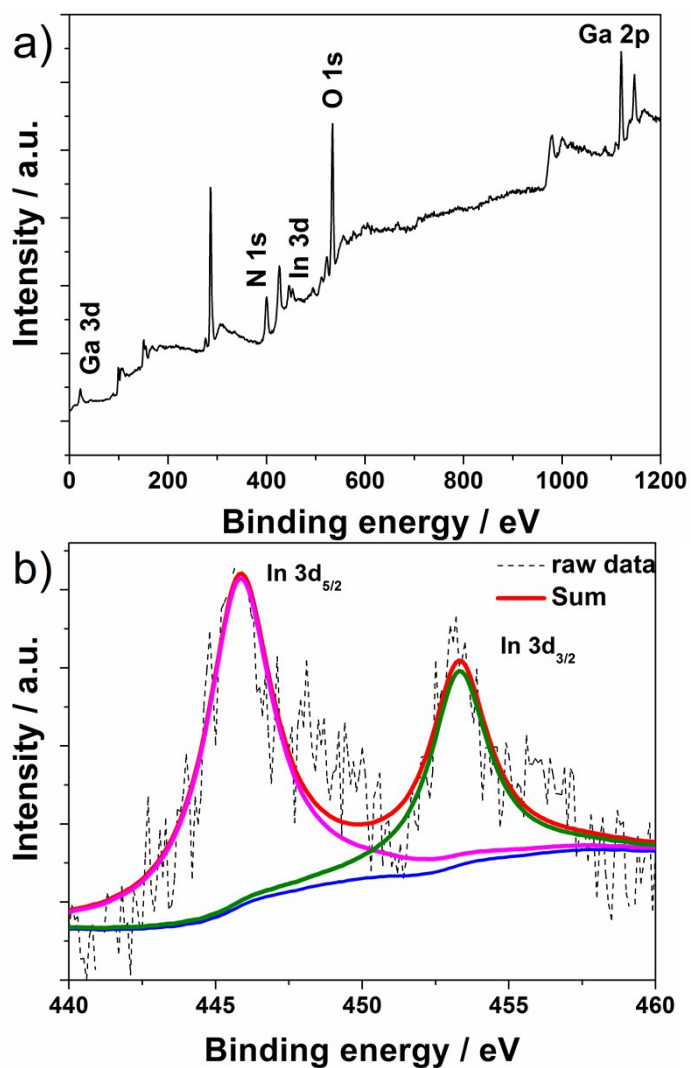


Figure S14. (a) XPS survey spectrum of the as-deposited In doped gallium nitride on Au electrode from the ternary molten electrolyte based on acetamide, urea and gallium nitrate. (b) represents high resolution In 3d core level spectrum.

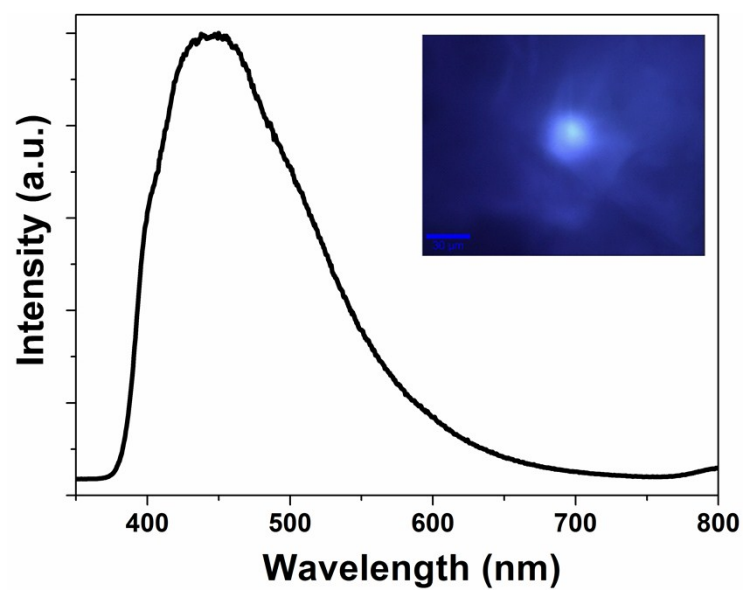


Figure S15. Room temperature photoluminescence spectrum of In doped gallium nitride/oxynitride under illumination of UV laser. The inset represents the CCD image of light emission observed on the flake upon illumination with UV laser.

Raman shift (cm ⁻¹)				
Acetamide	Urea	Ga(NO ₃) ₃	Ga(NO ₃) ₃ –based ternary melt	Band assignment
877			871	C-C & C-N stretch
1149			1136	NH rocking
1404	1469		1400	Amide III
1642	1623		1606	Amide II
		733	714	ν_4 bending
		1049	1047	ν_1 NO ₃ ⁻ symmetric
		1328	1356	NO ₂ symmetric
		1414	1434	ν_3 anti-symmetric

Table S1. FT-Raman band assignment for gallium nitrate containing ternary molten electrolyte along with the components.

Wavenumber (cm ⁻¹)				
Acetamide	Urea	Ga(NO ₃) ₃	Ga(NO ₃) ₃ based ternary melt	Band assignment
600-800	600-800		600-800	N-H out plane bending
1396			1389	C-N stretch
1452	1465		1447	C-N stretch
1668	1678		1651	C=O stretch
3180	3350		3196	N-H symmetric
3364	3441		3340	N-H anti-symmetric
		814	866	ν_4 NO ₃ ⁻
		1043	1045	ν_1 NO ₃ ⁻
		1305	1342	NO ₂ symmetric

Table S2. FT-IR band assignment for gallium nitrate containing ternary molten electrolyte along with the components.

References:

1. K. Kawaguchi, T. Ishiwata, E. Hirota, I. Tanaka, *Chem. Phys.* 1998, **231**, 193.
2. I. R. Lewis, H. Edwards, *Handbook of Raman Spectroscopy: From the Research Laboratory to the Process Line*. CRC Press: **2001**.
3. a) M. Kumar, B. Roul, T. N. Bhat, M. K. Rajpalke, A. T. Kalghatgi, S. B. Krupanidhi, *Jpn. J. Appl. Phys.* 2012, **51**, 020203; b) S. L. Hwang, K. S. Jang, K. H. Kim, H. S. Jeon, H. S. Ahn, M. Yang, S. W. Kim, Y. Honda, M. Yamaguchi, N. Sawaki, J. Yoo, S. M. Lee, M. Koike, *Phys. Stat. Sol. C* 2007, **4**, 125.
4. Z. Liliental-Weber, K. M. Yu, M. Hawkrige, S. Bedair, A. E. Berman, A. Emara, D. R. Khanal, J. Wu, J. Domagala, J. Bak-Misiuk, *Phys. Stat. Sol. C* 2009, **6**, 2626.